Int J Thermophys (2009) 30:1372–1385
DOI 10.1007/s10765-009-0595-1

Carbon Aerogel-Based High-Temperature Thermal Insulation

M. Wiener · G. Reichenauer · S. Braxmeier · F. Hemberger · H.-P. Ebert

Received: 15 October 2008 / Accepted: 13 May 2009 / Published online: 10 June 2009

Abstract Carbon aerogels, monolithic porous carbons derived via pyrolysis of porous organic precursors synthesized via the sol–gel route, are excellent materials for high-temperature thermal insulation applications both in vacuum and inert gas atmospheres. Measurements at 1773 K reveal for the aerogels investigated thermal conductivities of 0.09 $W \cdot m^{-1} \cdot K^{-1}$ in vacuum and 0.12 $W \cdot m^{-1} \cdot K^{-1}$ in 0.1 MPa argon atmosphere. Analysis of the different contributions to the overall thermal transport in the carbon aerogels shows that the heat transfer via the solid phase dominates the thermal conductivity even at high temperatures. This is due to the fact that the radiative heat transfer is strongly suppressed as a consequence of a high infrared extinction coefficient and the gaseous contribution is reduced since the average pore diameter of about 600 nm is limiting the mean free path of the gas molecules in the pores at high temperatures. Based on the thermal conductivity data detected up to 1773 K as well as specific extinction coefficients determined via infrared-optical measurements, the thermal conductivity can be extrapolated to 2773 K yielding a value of only 0.14 $W \cdot m^{-1} \cdot K^{-1}$ in vacuum.

Keywords Carbon aerogels · High temperature · Porous carbons · Thermal conductivity · Thermal insulation

1 Introduction

Carbon aerogels [1], i.e., porous carbons synthesized via the sol–gel route, are considered as very interesting materials for high-temperature thermal insulations in non-oxidizing atmospheres or vacuum [2–4]. Aerogels are open porous solids consisting of a

M. Wiener (✉) · G. Reichenauer · S. Braxmeier · F. Hemberger · H.-P. Ebert
Bavarian Center for Applied Energy Research, Am Hubland, 97074 Würzburg, Germany
e-mail: matthias.wiener@zae.uni-wuerzburg.de

three-dimensional network of spherical interconnected primary particles. The mean pore and particle size can be specifically adjusted to be in the range from several nanometers only to some microns by varying the synthesis conditions. Porosities up to about 99 % can be achieved. These properties make carbon aerogels suitable for thermal insulation applications [5], in particular at high temperatures, but also for electrodes in supercapacitors [6–8] and gas diffusion layers in fuel cells [9,10].

Wiener et al. [5] showed that the thermal conductivity via the backbone of carbon aerogels is strongly increasing with the pyrolysis or the annealing temperature applied; this is due to the increase in ordering of the carbon structure on the molecular scale accompanied by the growth of the carbonaceous microcrystallites. The study revealed that these structural changes mainly reduce the grain boundaries and thus the scattering of the phonons dominating the heat transport via the solid phase. In contrast, the electronic contribution to the thermal transport was shown to be negligible as expected for highly amorphous systems. Nevertheless, the earlier paper already revealed the high potential of carbon aerogels as high-temperature thermal insulations.

In the present study, the total effective thermal conductivity of two carbon aerogels was determined as a function of temperature in argon as well as under vacuum to investigate the different contributions to the overall heat transfer.

2 Heat Transfer in Carbon Aerogels

In general, the total effective thermal conductivity, λ_{eff}, of porous materials such as carbon aerogels comprises at least three contributions: the thermal conductivity of the solid backbone, λ_{s}, the contribution of the gaseous phase, λ_{g}, and the radiative thermal conductivity, λ_{r}. To a good approximation the total effective thermal conductivity can be described by a superposition of the three contributions [11]:

$$\lambda_{\mathrm{eff}} = \lambda_{\mathrm{s}} + \lambda_{\mathrm{g}} + \lambda_{\mathrm{r}}. \tag{1}$$

At room temperature and above, the heat transfer in solids, λ_{s}, is a diffusive transport via phonons; in case of electrically conductive materials, an additional contribution due to heat transfer via electrons can be relevant. Wiener et al. [5] showed that for carbon aerogels the contribution of the electrons to the thermal conductivity is negligible. Therefore, the solid thermal conductivity in aerogels can be described by the phonon diffusion model [12]:

$$\lambda_{\mathrm{s}} = \frac{1}{3} c_v \rho v_{\mathrm{ph}} l_{\mathrm{ph}}, \tag{2}$$

where $c_v \approx c_p$ is the specific heat at constant volume, ρ is the sample density, v_{ph} is the mean velocity of the phonons, and l_{ph} is the mean free path of the phonons. At the temperature relevant within the framework of this study, the mean free path of the phonons, however, is controlled by the molecular order in the solid phase of the sample investigated and thus is affected by the pyrolysis temperature [5]. On the other hand, the specific heat depends on the specimen temperature. Consequently,

λ_s is a function of the measurement temperature T as well as a function of the pyrolysis temperature T_{pyro}.

The gaseous thermal conductivity in porous media can be calculated via [13]

$$\lambda_g(T) = \frac{\Pi \lambda_{g,0}(T)}{(1 + 2\beta Kn)}, \tag{3}$$

where $\lambda_{g,0}$ is the thermal conductivity of the free gas, Π is the porosity of the material, β is a constant including the interaction between the gas molecules and the pore walls, and Kn is the Knudsen number which is defined as the ratio of the mean free path of the gas molecules l_g and the pore size D: $Kn = l_g/D$. Convection within the carbon aerogels can be neglected for the material structure and environmental conditions given.

The mean free path of the gas molecules is a function of the temperature according to

$$l_g(T) = \frac{k_B T}{\sqrt{2\sigma_0} p_g}, \tag{4}$$

with k_B is the Boltzmann constant, σ_0 is the cross section of the molecule, and p_g is the gas pressure. The thermal conductivity of the free gas can be calculated via the kinetic theory of gases according to [14]

$$\lambda_{g,0}(T) = \frac{2c_v}{3\sigma_0}\sqrt{\frac{k_B T}{\pi m}}, \tag{5}$$

where c_v is the specific heat of the gas at constant volume and m is the mass of the respective gas molecule or atom.

For optically thick media, the radiative heat transfer can be considered as a diffusion process, and to a good approximation, calculated by

$$\lambda_r = \frac{16 n^2 \sigma_B}{3\rho e(T)} T^3. \tag{6}$$

Here n is the complex index of refraction of the material, σ_B is the Stefan-Boltzmann constant, ρ is the sample density, and e is the specific extinction coefficient.

3 Experimental

3.1 Carbon Aerogel Synthesis

The carbon aerogels investigated in this work were derived via pyrolysis of organic aerogel precursors. The precursors were synthesized according to the sol–gel process which is described in detail elsewhere [15]. Briefly, an aqueous solution of resorcinol and formaldehyde was mixed; hereby the dilution of the reactants resorcinol and formaldehyde in the starting aqueous solution was adjusted to a mass ratio M of 25 % (M = mass of resorcinol and formaldehyde to total mass of the solution) to yield a

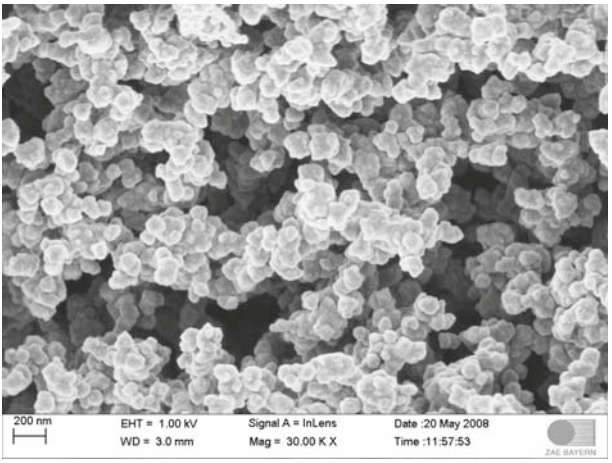

Fig. 1 SEM image of one of the carbon aerogels synthesized ($T_{\text{pyro}} = 2073\,\text{K}$)

density of the resulting aerogel of about $230\,\text{kg} \cdot \text{m}^{-3}$. Then sodium carbonate was added as a base catalyst. The amount of catalyst controls the particle growth during the chemical reaction and thus the size and specific surface area of the backbone forming particles; at a given porosity of the aerogel, the catalyst concentration, therefore, also determines the average pore size. The molar ratio of resorcinol to catalyst was set to 2000 to provide an average pore size of the final carbon aerogel of about 550 nm.

The solution was filled in cylindrical glass vessels and sealed airtight. Then the samples were exposed to 85 °C for 24 h [15] for gelling and curing. Afterwards, the pore liquid within the wet gel was replaced by ethanol to reduce the surface tension upon drying. Subsequently, the gels were dried at ambient conditions. Finally the resulting organic aerogels were pyrolyzed in an argon atmosphere at 1073 K and 2073 K. Figure 1 shows the microscopic structure of one of the carbon aerogels synthesized.

3.2 Measurement of the Specific Heat

The specific heat $c_p(T)$ of the carbon aerogels was determined by differential scanning calorimetry (DSC) measurements using a DSC 404 C (Netzsch Gerätebau GmbH, Germany). The measurements were performed in a temperature range from about 303 K to 1773 K in argon atmosphere. The temperature ramp was $10\,\text{K} \cdot \text{min}^{-1}$. The sample holders used were crucibles made of a platinum body and an alumina insert. The inner diameter of the crucible was 5 mm. The low-density aerogel was milled and then compressed into a pellet of 5 mm in diameter to provide a maximum loading of the crucible and reasonable heat transfer for the DSC measurement. The resulting sample mass was about 8 mg.

3.3 Determination of the Thermal Conductivity

The total effective thermal conductivities λ_{eff} of the samples were calculated from the thermal diffusivity a according to

$$\lambda_{\text{eff}} = a(T)\rho c_p(T), \tag{7}$$

where c_p is the specific heat at constant pressure and ρ is the density of the sample. The thermal diffusivities were derived via standard laser-flash measurements. The front side of the sample was hereby heated via a laser pulse (NdYaG-Laser, wavelength = 1064 nm; pulse length = 0.3 ms), and the temperature at the backside of the sample was monitored by an infrared detector as a function of time. From the time dependence of the signal, the thermal diffusivity a can be calculated. A more detailed analytical description can be found in [16]. The laser-flash apparatus applied is equipped with a furnace allowing temperature dependent measurements up to 1773 K. Additionally, measurements can be performed under vacuum and inert gases at different gas pressures, respectively.

For the laser-flash measurements, the carbon aerogel specimens were cut with a diamond saw to provide discs with a diameter of 12 mm and a thickness of 500 μm.

3.4 Determination of the Specific Extinction Coefficient

The specific extinction coefficients e of the carbon aerogel specimens were determined in the infrared-optical wavelength regime using a Fourier transform infrared spectrometer (Bruker IFS 66 v). Earlier investigations showed that the extinction of carbon aerogels is dominated by absorption [5]. The carbon aerogel samples were therefore characterized by measuring the directional-directional transmittance T_{dd} at ambient temperature for wavelengths between 1.5 μm and 40 μm.

Normally, the specimens used for this kind of measurement are prepared as fine powders embedded in a highly dispersed form in a KBr tablet. However, for the case of carbon aerogels the porous monolithic specimen itself acts as an optical absorber; in that case the arrangement of the carbon within the sample is crucial for the mass being effective. We therefore tried to prepare a monolithic aerogel sample for the absorption measurement. However, because of the strong absorbance of the carbon aerogel and the limited sensitivity of the FTIR spectrometer, a layer of only a few tens of microns is required. To meet these demands, a thin aerogel slice was prepared by attaching a piece of Scotch tape onto the aerogel surface and then stripping it off together with a thin detached layer of the carbon aerogel surface. For the measurement the sample including the supporting Scotch tape (thickness $\approx$ 50 μm) was placed directly into the beam with its surface normal to the direction of the beam. The measured spectrum was then corrected for the spectrum of the Scotch tape only.

From the resulting transmittance spectrum, the extinction coefficient was calculated as a function of wavelength using Beer's law. In order to deduce the extinction coefficient as a function of temperature, the spectral extinction coefficient was weighted using the Rosseland averaging function [17].

3.5 Characterization of the Aerogel Morphology

The structure of the carbon aerogels investigated was characterized by nitrogen sorption measurements at 77 K using a Micromeritics ASAP 2000 apparatus. Prior to

sorption analysis, each sample was degassed at 300 °C under vacuum for at least 12 h.

The measured isotherm was evaluated with respect to the total and external specific surface area. The total surface area S_{BET} of the carbon aerogel was derived by using the BET (Brunauer–Emmert–Teller) analysis [18] in the relative pressure range between $p/p_0 = 0.05$ and 0.26; to determine the envelope surface area of the backbone particles only, the so-called specific external surface area S_{ext} was determined via a t-plot [19].

The mean pore size D was calculated from the specific external surface area, S_{ext}, under the assumption that the pore geometry is cylindrical:

$$D = \frac{4V_{\mathrm{pore}}}{S_{\mathrm{ext}}} \tag{8}$$

V_{pore} is hereby the specific volume of the pores in between the backbone particles, it is calculated from the density of the specimen ρ and the particle density ρ_{part}:

$$V_{\mathrm{pore}} = \frac{1}{\rho} - \frac{1}{\rho_{\mathrm{part}}}. \tag{9}$$

The density of the microporous carbon particles was hereby assumed to be 1400 kg · m^{-3}. The mean particle size d is related to the specific external surface area and the particle density by

$$d = \frac{6}{S_{\mathrm{ext}}\rho_{\mathrm{part}}}. \tag{10}$$

4 Experimental Results

4.1 Morphology

The mean particle and pore sizes of the carbon aerogels investigated were determined from nitrogen sorption data according to Eqs. 8–10. The mean particle and pore diameters calculated are given in Table 1 together with the densities, specific pore volumes, and specific surface areas of the two specimens. The values reveal that the morphology of the carbon aerogels exposed to different annealing temperatures is very similar for length scales on the order of the particle size and above. The data derived for the particle size were confirmed by visual analysis of the SEM image (Fig. 1).

Only the comparison of the BET surface areas indicates that the structure within the particles, i.e., the micropores and microcrysallites are affected by the pyrolysis temperature. With a higher pyrolysis temperature the micropores become wider and increasingly inaccessible [20].

Table 1 Structural characteristics of two different carbon aerogels investigated

Pyrolysis/annealing temperature (K)	Density ($kg \cdot m^{-3}$)	Pore volume V_{pore} ($cm^3 \cdot g^{-1}$)	Specific external surface area S_{ext} ($m^2 \cdot g^{-1}$)	S_{BET} ($m^{-2} \cdot g^{-1}$)	Mean pore diameter (nm)	Mean particle diameter (nm)
2073 ± 20	225 ± 9	3.7 ± 0.4	28 ± 2	38 ± 2	529 ± 106	153 ± 14
1073 ± 10	225 ± 9	3.7 ± 0.4	25 ± 2	575 ± 29	592 ± 118	171 ± 15

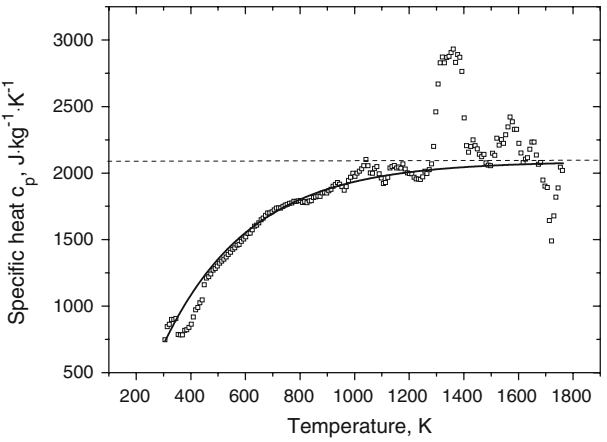

Fig. 2 Experimental data of the specific heat including underlying reaction enthalpies for a carbon aerogel pyrolyzed/annealed at 1973 K (*open square*), *full line* corresponds to a fit of Eq. 11 to the data, and *dashed line* marks the upper limit of the specific heat according to Dulong-Petit

4.2 Specific Heat

Figure 2 shows the measured data of the specific heat c_p and underlying reaction enthalpies for a carbon aerogel pyrolyzed/annealed at 1973 K in the temperature range from about 300 K to 1800 K. The pyrolysis temperature of the aerogel under investigation was well beyond the maximum temperature of the caloric measurement in order to prevent changes in structure during the measurement. The strong fluctuations of the data for temperatures beyond 1300 K can be ascribed to chemical reactions between the specimen and the crucible.

For further calculations, it is handy to have an analytical equation that describes the specific heat as a function of the temperature and approaches the Dulong-Petit limit at high temperatures. A suitable function is

$$c_p(T) = -P1 + P2\left(1 - \exp\left(-\frac{T}{P3}\right)\right); \tag{11}$$

a fit of this relation to the experimental data, yields the parameters $P1 = 1440$ $J \cdot kg^{-1} \cdot K^{-1}$, $P2 = 3528\,J \cdot kg^{-1} \cdot K^{-1}$, and $P3 = 319\,K$.

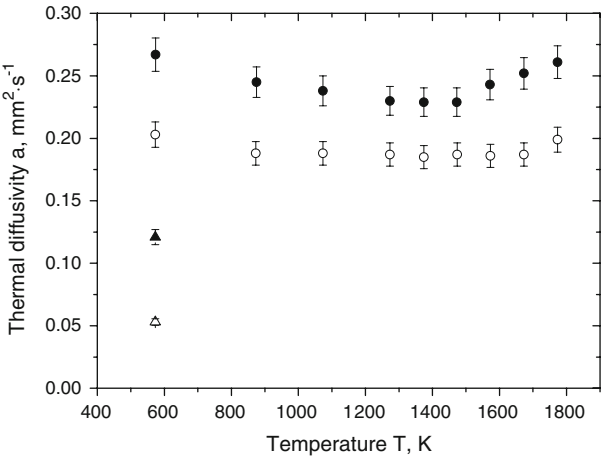

Fig. 3 Thermal diffusivity of a carbon aerogel (pyrolysis temperature = 2073 K) as a function of temperature under 0.1 MPa argon atmosphere (*filled circle*) and vacuum (*open circle*). Values for a carbon aerogel (pyrolysis temperature = 1073 K) at 573 K in 0.1 MPa argon atmosphere (*filled triangle*) and vacuum (*open triangle*)

4.3 Thermal Diffusivity

Figure 3 shows the thermal diffusivities for the two carbon aerogels as measured via the laser-flash technique at different temperatures up to 1773 K in argon and under vacuum. Hereby, the aerogel pyrolyzed at 1073 K was measured at 573 K only. In both cases the pyrolysis temperature exceeded the maximum temperature applied during the measurement. This way irreversible changes of the samples during the measurement were avoided.

4.4 Infrared Extinction

Figure 4 shows the specific extinction coefficient as a function of the wavelength and the corresponding data as a function of temperature. The two curves refer to two separately but similarly prepared samples of the same carbon aerogel ($T_{\text{pyro}} = 2073$ K). The difference of the data results from the preparation. A check of the homogeneity of the sample layer was performed by measuring its dimensions and mass (see Table 2), calculating its density, ρ_{layer}, and comparing it to the density of the aerogel monolith, ρ. The discrepancy of these data for the case of preparation 2 shows that the material in the layer is not homogeneously distributed. Preparation 1 is therefore classified as more reliable, and the corresponding data are used for the following calculations.

5 Discussion

The effective thermal conductivities as calculated according to Eq. 7 from the determined values of thermal diffusivity $a(T)$, specific heat $c_p(T)$, and sample densities ρ are shown for the two carbon aerogels investigated in Fig. 5.

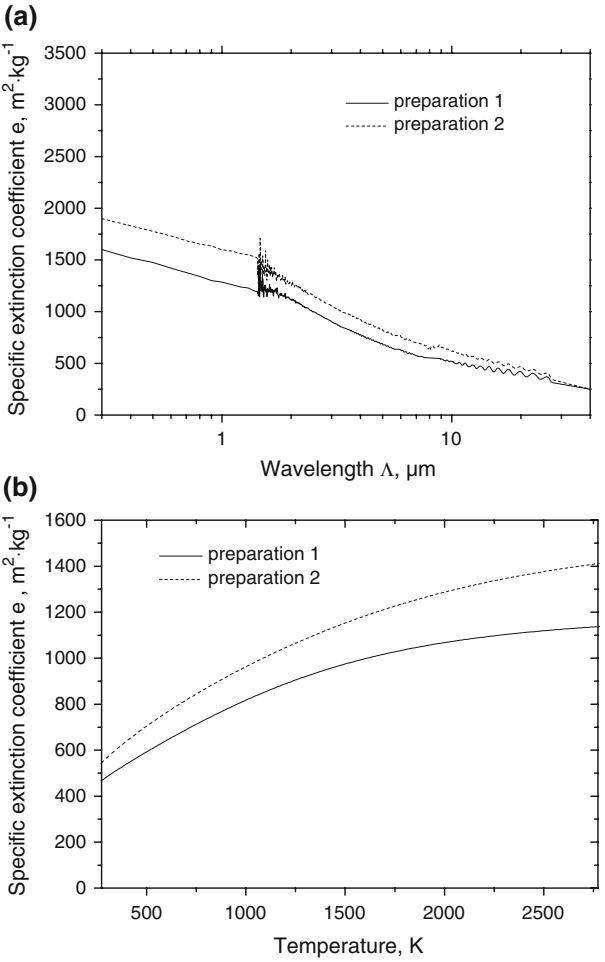

Fig. 4 Specific extinction coefficients of the carbon aerogel annealed at 2073 K as a function of (**a**) wavelength and (**b**) temperature. *Curves* represent two separate preparations of the same specimen

The comparison of the values derived in 0.1 MPa argon atmosphere and under vacuum shows that the difference between the two datasets (see Fig. 6) is almost temperature independent on the order of $0.02\,\mathrm{W}\cdot\mathrm{m}^{-1}\cdot\mathrm{K}^{-1}$. This difference in thermal conductivities represents the contribution of the gas in the pores of the aerogel to the total effective thermal conductivity. Compared to the values expected for the thermal conductivity of free argon weighted by the porosity of the specimen, the thermal conductivity is significantly suppressed for temperatures above about 1000 K (see Fig. 6). The mean free path of argon atoms at 1000 K is about 230 nm, a value that is only a factor of two smaller than the average pores size of the specimens (Table 1). This corresponds to a Knudsen number *Kn* of 0.5, a value for which the theoretical gaseous thermal conductivity as given by Eq. 3 is significantly reduced compared to the one for the free gas. According to Eqs. 3–5, the temperature dependence of the gaseous thermal conductivity, λ_g, in porous media is given by

Table 2 Data of two carbon aerogel samples prepared from the same specimen as an adhesive layer on Scotch tape (diameter = 15 mm)

	ρ_{monolith} ($\text{kg} \cdot \text{m}^{-3}$)	d_{layer} (μm)	d_{scotch} (μm)	ρ_{scotch} ($\text{kg} \cdot \text{m}^{-3}$)	ρ_{layer} ($\text{kg} \cdot \text{m}^{-3}$)	$(\rho_{\text{layer}} - \rho_{\text{monolith}}/\rho_{\text{monolith}})\,100\,(\%)$
Preparation 1	225 ± 9	23 ± 2	50 ± 2	1029 ± 42	223 ± 9	0.9
Preparation 2	225 ± 9	25 ± 2	50 ± 2	1029 ± 42	207 ± 9	8.0

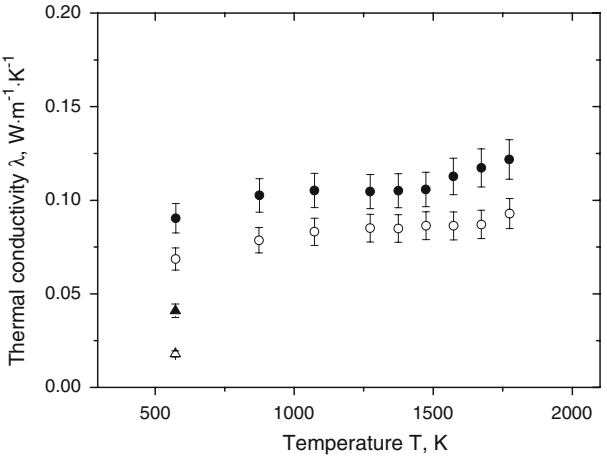

Fig. 5 Thermal conductivity of the investigated carbon aerogel (pyrolysis temperature = 2073 K) as a function of temperature under 0.1 MPa argon atmosphere (*filled circle*) and vacuum (*open circle*). Also shown is the thermal conductivity of a carbon aerogel (pyrolysis temperature = 1073 K) at 573 K in 0.1 MPa argon atmosphere (*filled triangle*) and vacuum (*open triangle*)

$$\lambda_g(T) \propto \frac{\sqrt{T}}{1 + C\frac{T}{D}}, \tag{12}$$

where C is a material specific constant. Since the second term in the denominator of Eq. 12 is larger than 1 for 1000 K and further increases with temperature the gaseous contribution to the thermal conductivity for the carbon aerogel under investigation is expected to decrease in the high temperature limit with $T^{-0.5}$; this is due the fact that for Knudsen numbers >1, the temperature dependence of the mean free path of the gas is overcompensating the increase of the thermal conductivity of the free gas with temperature.

According to Eq. 1, the effective thermal conductivities measured under vacuum represent the superposition of the thermal conductivity via the solid phase and radiative heat transfer. To quantify the contribution of the two terms, the radiative thermal conductivity was calculated via Eq. 6 using the extinction coefficient $e(T)$ shown in Fig. 4b; hereby a refractive index $n = 1.1$ was used, which had been calculated according to the Clausius-Mossotti formula [22].

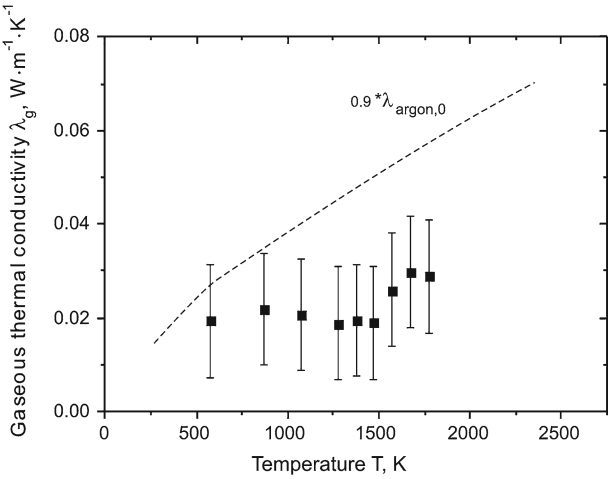

Fig. 6 Gaseous contribution, λ_g, to the total effective thermal conductivity of the carbon aerogel pyrolyzed at 2073 K as a function of temperature (*filled square*). Data were derived from the difference of the measurements under argon atmosphere and vacuum (see Fig. 5). In addition, literature data of the thermal conductivity for free argon gas [21] for a porosity of 90 % are depicted (*dashed line*)

$$\frac{n^2-1}{n^2+2} = (1-\Pi)\frac{n_s^2-1}{n_s^2+2} + \Pi\frac{n_p^2-1}{n_p^2+2}, \tag{13}$$

where n_s is the refractive index of the solid ($n_{carbon} = 2$) and n_p is the refractive index of the pores ($n_{air} = 1$). $(1-\Pi)$ and Π are the fractions of the solid and pores in the material, respectively. The theoretical values derived for the radiative thermal conductivity as a function of temperature are plotted in Fig. 7.

In Fig. 8 these data are compared to the experimental data of the total effective thermal conductivities measured in vacuum. The plot reveals that the radiative transport represents even at 1770 K only a small contribution to the total effective thermal conductivity in the carbon aerogel investigated. The thermal transport is rather dominated by the heat transfer via the solid phase. The full line in Fig. 8 corresponds to a fit of a superposition of the radiative thermal conductivity and the solid thermal conductivity as given by the phonon diffusion model (Eq. 2) with the product of l_{ph} and v_{ph} as a free parameter. The plot shows that the temperature dependence of the total effective thermal conductivity at temperatures below about 1200 K is well-represented by the temperature dependence of the specific heat (see Fig. 2). The theoretical values are plotted only up to the temperature of 2073 K, i.e., the temperature that the sample has already been exposed to upon pyrolysis.

Figure 5 shows, the heat treatment temperature (T_{pyro}) is a crucial parameter in terms of the solid thermal conductivity of the aerogel. At a measurement temperature of 573 K, the thermal conductivity shifts from 0.018 $W \cdot m^{-1} \cdot K^{-1}$ for the aerogel pyrolyzed at 1073 K to 0.068 $W \cdot m^{-1} \cdot K^{-1}$ for the aerogel derived from the same

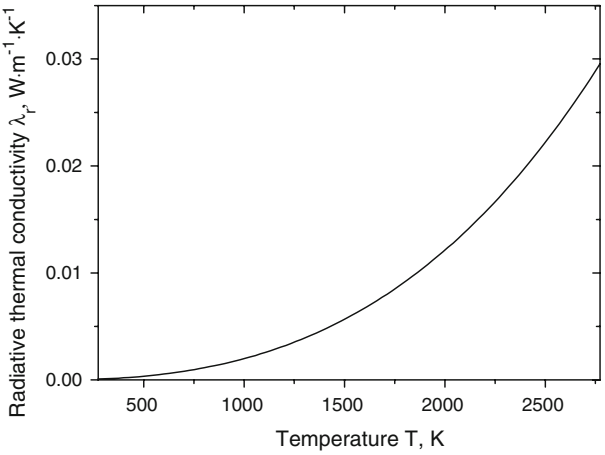

Fig. 7 Radiative contribution to the thermal conductivity of the carbon aerogel pyrolyzed at 2073 K as a function of temperature; values were calculated via Eq. 6 from the data shown in Fig. 4 for preparation run 1

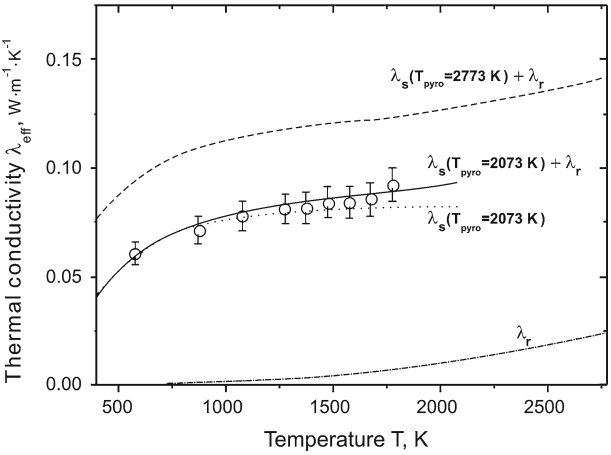

Fig. 8 Thermal conductivities of a carbon aerogel (pyrolysis temperature = 2073 K) measured as a function of temperature in vacuum (*open circle*). Radiative λ_r and solid λ_s contributions to the thermal conductivity are indicated; *full line* represents the superposition of the two terms. *Upper dashed line* corresponds to the thermal conductivity expected for the same aerogel, however, pyrolyzed at 2773 K

organic precursor, however, with a pyrolysis temperature of 2073 K. Assuming a linear increase of the solid thermal conductivity with the pyrolysis temperature as reported in Ref. [5] the shift in thermal conductivity for an aerogel pyrolyzed at 2773 K compared to the experimental data shown in Fig. 8 is expected to be $0.035\ W \cdot m^{-1} \cdot K^{-1}$. The upper dashed line in Fig. 8 represents the effective thermal conductivity to be expected for a carbon aerogel derived from the same organic precursor as the samples measured here, however, pyrolyzed at a temperature of 2773 K. Under 0.1 MPa argon

atmosphere, the values are expected to increase by an additional constant term of about $0.02\,\mathrm{W}\cdot\mathrm{m}^{-1}\cdot\mathrm{K}^{-1}$.

6 Conclusions and Outlook

The total effective thermal conductivity of the ambient pressure dried carbon aerogel investigated with a density as low as $225\,\mathrm{kg}\cdot\mathrm{m}^{-3}$ and an average pore size of about 600 nm possesses an ultra-low thermal conductivity of only about $0.12\,\mathrm{W}\cdot\mathrm{m}^{-1}\cdot\mathrm{K}^{-1}$ at a temperature of about 2000 K in 0.1 MPa argon atmosphere. Extrapolations of the data to temperatures of 2700 K yield maximum effective total thermal conductivities of about $0.16\,\mathrm{W}\cdot\mathrm{m}^{-1}\cdot\mathrm{K}^{-1}$. These values are a factor of five to ten lower than the ones for established high-temperature thermal insulation materials like carbon fiber felts or carbon foams currently available. Therefore, carbon aerogels are expected to be excellent candidates for applications within this field. In contrast to carbon fibers and foams, the thermal conductivity increases only moderately with temperature. Essential for this characteristic property is the adjustable morphology of aerogel, which allows suppressing the gaseous thermal conductivity by the appropriate pore size on the one hand and reducing the radiative thermal heat transfer effectively on the other hand.

The study shows that it is still very difficult to provide reliable data for the infrared extinction coefficient for highly absorbing materials like carbon aerogels. Consequently, the sample preparation method for the IR-optical measurements needs to be improved to provide acceptable uncertainties for the extinction data.

Further reduction of the total effective thermal conductivity could be achieved by modifying the chemistry of the solid backbone. This topic will be investigated in the near future.

References

1. R.W. Pekala, J. Mater. Sci. **24**(9), 3221 (1989)
2. V. Bock, O. Nilsson, J. Blumm, J. Fricke, J. Non-Cryst. Solids **185**(3), 233 (1995)
3. L.W. Hrubesh, R.W. Pekala, J. Mater. Res. **9**(3), 731 (1994)
4. X.P. Lu, O. Nilsson, J. Fricke, R.W. Pekala, J. Appl. Phys. **73**(2), 581 (1993)
5. M. Wiener, G. Reichenauer, F. Hemberger, H.-P. Ebert, Int. J. Thermophys. **27**(6), 1826 (2006)
6. H. Proebstle, M. Wiener, J. Fricke, J. Porous. Mat. **10**(4), 213 (2003)
7. U. Fischer, R. Saliger, V. Bock, R. Petricevic, J. Fricke, J. Porous. Mat. **4**, 281 (1997)
8. W.C. Li, G. Reichenauer, J. Fricke, Carbon, **40**(15), 2955 (2002)
9. M. Glora, M. Wiener, R. Peticevic, H. Pröbstle, J. Fricke, J. Non-Cryst. Solids **285**(1–3), 283 (2001)
10. R. Petricevic, M. Glora, J. Fricke, Carbon **39**(6), 857 (2001)
11. J. Fricke, High Temps. - High Press. **25**, 379 (1993)
12. P. Debye, *Vorträge uber die kinetische Theorie der Materie und der Elektrizitat* (Teubner, Berlin, 1914)
13. M.G. Kaganer, *Thermal Insulation in Cryogenic Engineering* (IPST Press: Jerusalem, Israel, 1969)
14. F. Reif, H.L. Scott, Am. J. Phys. **66**, 164 (1998)
15. M. Wiener, G. Reichenauer, T. Scherb, J. Fricke, J. Non-Cryst. Solids **350**, 126 (2004)
16. H.S. Carslaw, J.C. Jaeger, *Conduction of Heat in Solids* (Oxford Science Publications, Oxford, 1995)
17. R. Siegel, J.R. Howell, *Thermal Radiation heat transfer* (McGraw-Hill Kogakushka, Ltd., Tokyo, 1972)
18. S. Brunauer, P.H. Emmett, E. Teller, J. Am. Chem. Soc. **60**(2), 309 (1938)
19. S.J. Gregg, K.S.W. Sing, *Adsorption, Surface Area and Porosity*, 2nd edn. (Academic Press, London, 1982)
20. Y. Hanzawa, H. Hatori, N. Yoshizawa, Y. Yamada, Carbon **40**(4), 575 (2002)

21. Y.S. Touloukian, P.E. Liley, S.C. Saxena, *Thermal Conductivity - Nonmetallic Solids*, vol. 2 (Plenum Publishing Co., New York, 1970)
22. J.D. Jackson, R.F. Fox, Classical Electrodynamics, Am. J. Phys. **67**, 841 (1999)